Journal of Molecular Structure 1241 (2021) 130701

Contents lists available at ScienceDirect

Journal of Molecular Structure

journal homepage: www.elsevier.com/locate/molstr

Azolium mediated N–Heterocyclic carbene selenium adducts: Synthesis, cytotoxicity and molecular docking studies

Rizwan Ashraf[a,1,*], Zohra Khalid[a], Ayesha Sarfraz[a], Haq Nawaz Bhatti[a], Muhammad Adnan Iqbal[a], Mansoureh Nazari V[b]

[a] Department of Chemistry, University of Agriculture Faisalabad, Pakistan
[b] School of Pharmacy, University August 17, 1945 14350 Jakarta, Indonesia

ARTICLE INFO

Article history:
Received 17 November 2020
Revised 21 April 2021
Accepted 8 May 2021
Available online 19 May 2021

Keywords:
Ionic Liquids
N-Heterocyclic Carbenes (NHCs)
Selenium compounds
Molecular docking
Anticancer studies

ABSTRACT

Ionic liquids (ILs) are remarkable for biological activities in numerous medical fields. With the aim of enhancing biological potential of azolium based ILs, four new selenium-N-Heterocyclic Carbene (Se-NHC) adducts were synthesized from bis-imidazolium and bis-benzimidazolium molten salts. Synthesized ILs (**L_1-L_4**) and Se-NHC adducts (**C_1–C_4**) were confirmed through elemental analysis, chromatographic and spectroscopic techniques including UHPLC-PDA, FTIR, ^{1}H NMR & ^{13}C NMR spectroscopy as well as mass spectrometry. The compounds were found stable in solution form for upto 96 h measured spectroscopically and showed partition coefficient with optimum lipophilicity measured through shake flask method. The simulation studies of these compounds for cancerous proteins indicated that there could be good to high anticancer potential due to their high affinity and less binding energies for COX-1, EGF, VEGF-A and HIF cancer protein targets. The *In Vitro* cytotoxicity study of compounds confirmed that these compounds were found highly active showeing IC_{50} against HCT-116 (1.074–1.116 μg mL^{-1}), A549 (0.977–1.325 μg mL^{-1}) and MCF-7 (0.869–1.378 μg mL^{-1}) which is almost better than standard drug 5-Flourouracil but slightly lower than cisplatin and oxaliplatin. The interaction study of compounds with albumin proteins (BSA) and hemolysis assay assured their least toxicity.

Introduction

Medicinal inorganic chemistry is a growing interdisciplinary area of chemical research which showed substantial progress in diagnostics and cancer treatment [1]. In this continuation, development of cis-platin and its analogues were a lead to combat various types of cancers but its use was hampered due to growing resistance and serious side effects [2]. Therefore, extensive efforts are carried out in the search of new organometallics with minimum side effects and interestingly, some non-platinum analogues offered promising features to replace resistant class of chemo drugs. In particular, there are reports indicating that organo-selenium compounds are best fit having substantial ability to modulate multiple physiological pathways as well as being essential trace element for various body mechanisms [3]. Although selenium could be toxic in higher amount but its controlled amount is safe as well as essential for cell metabolism of sleno-proteins like thioredoxinreductase, glutathione peroxidase etc. involved in maintenance of antioxidant functions [1,3,4].

Although various *In vitro* studies indicated that selenium based compounds showed good anticancer potential [5] but, its efficacy is very much dependent upon bioavailability at its targeted site. Its bioavailability at target site is very dependent on rate of ionization, delivery route as well as its lipophilicity [6]. This entire scenario calls for a class of ligands that could be tuned for these properties in a wake of required drug development. Different researchers use versatile approaches to synthesize selenium adducts and the recent years have seen an emergence of N-heterocyclic carbenes (NHCs) as class of ligands that can be structurally tuned to make fit for drug design [7]. Imidazole and benzimidazole could results in ionic liquids (ILs) with tunable structure to generate NHCs compound [8]. The steric and electronic tunability is an additional feature of these ILs that affect the stability while complexing through strong σ-donor properties which can be customized by substituents at the nitrogen atoms as well as at the carbon backbone of the heterocyclic skeleton that optimized the coordination of ILs with metal center and affects the lipophilicity, stability and ultimately efficacy of drug [9]. The molten salts were reported for their widespread applications including catalysis, extraction, biodiesel, solar cell as

* Corresponding author.
E-mail address: rizi_chem82@hotmail.com (R. Ashraf).
[1] Dedications: Authors dedicate this article to the memories of Dr. Bushra Sultana (late).

https://doi.org/10.1016/j.molstruc.2021.130701
0022-2860/

well as biological significances [10,11]. These biological applications of ILs can be improved through incorporation of elemental selenium in their organic frameworks.

Therefore, present study is planned for the synthesis of four ILs (L_1-L_4) and development of selenium adducts (C_1–C_4) from these molten salts and screened for their anticancer potentials. The solubility and stability of synthesized compounds were also investigated which is an important parameter of drug safety and efficacy. Furthermore, affinity of compunds (C1-C4) for serum albumins was tested, since drug albumin affinity plays very important role in drug distribution and its pharmacokinetics that influence *In vitro* half-life and extravasation of drug at the target site.

Materials and methods

All the chemicals including imidazole, Benzimidazole, Benzyl Bromide, 3-methyl butyl bromide and 1,2-dibromoethane were procured from Alfa Aesar, Ward Hill, Massachusetts, United States through local supplier Musaji Adam & sons Pakistan. Elemental selenium powder was purchased from Avonchem, United Kingdom through local supplier UH-Analytics Pakistan. The solvents used, Dimethyl sulfoxide (DMSO), Methanol, 1, 4-dioxane, n-hexane, petroleum ether were of analytical grade and used as they were procured from Merck (Darmstadt, Germany). Synthesized Precursors, ILs and their selenium compounds were characterized through FTIR (IRTracer-100, Shimadzu Japan) with post run processing software Lab solutions. UV–visible spectra of salts and their selenium compounds were measured through Shimadzu UV-1800 UV/Visible Scanning Spectrophotometer. All precursors and ligands were characterized through UHPLC-PDA/ESI-MS (Waters, USA) equipped with Empower 3.0 software to acquire UV–visible and mass spectra. ^{1}H & ^{13}C NMR spectra were acquired on Bruker–Avance NMR spectrometer using internal standard (TMS).

*Synthesis of 1-benzyl-1H-benzo[*d*]imidazole (I)*

Benzimidazole (2 g, 6.9 mmol) and KOH (1.4 g, 10.3 mmol) in 25 ml of DMSO stirred for 30 min followed by the addition of benzyl bromide (1.2 g, 6.9 mmol) and continued stirring for 5 h at room temperature. Reaction mixture was poured in chilled water and product was extracted with chloroform and solvent was evaporated through rotary evaporator. Yield: 89.3%. FT-IR (ATR cm^{-1}): 3075 (C–H str), 1624 (*C = C* str), 1429 (C–C str), 1203, 1188 (C–N str), 935 (*C = C* str), 673, 669 (C–H ben). UV-Visible (λ_{max}nm): 248.6, 212.0. MS (*m/z*): Predicted [M-1]$^+$, $[C_{14}H_{11}N_2]^+$= 207.12 Da, Found 207.10 Da.

Synthesis of 1-benzyl-1H-imidazole (II)

Imidazole (1.0 g, 14.7 mmol) and KOH (1.2 g, 22 mmol) in 25 ml of DMSO stirred for 30 min followed by addition of benzyl bromide (2.5 g, 14.7 mmol) and stirred for 5 h at room temperature. Product was separated by following he same method as followed for I. Yield: 82.7%. FT-IR (ATR cm^{-1}): 3082 (C–H str), 1614 (*C = C* str), 1493, 1452 (C–C str), 1286, 1265 (C–N str), 974, 935 (*C = C* str), 775, 745 (C–H ben). UV-Visible (λ_{max}nm): 258.1, 223.8. MS (*m/z*): Predicted $[M + 1]^+$, $[C_{14}H_{11}N_2]^+$= 159.05 Da, Found $[M + 1]^+$158.97 Da.

*Synthesis of 1-isopentyl-1H-benzo[*d*]imidazole (III)*

Benzimidazole (2.0 g, 6.9 mmol) and KOH (1.4 g, 10.3 mmol) in 25 ml of DMSO stirred for 30 min followed by the addition of 1–bromo-3-methylbutane (1.0 g, 6.9 mmol) and stirring continued for 5 h at room temperature. Reaction mixture was poured in cooled water and product was extracted through chloroform. Yield:79.7%. FT-IR (ATR cm^{-1}): 3246, 3237 (C_{arom}-H str), 2869 (C_{aliph}-H str), 1494 (C–C str), 1332, 1286 (C–N str), 974 (C–H ben). UV-Visible (λ_{max}nm): 274.8, 254.6 212.0. MS (*m/z*): Predicted $[M + 1]^+$, $[C_8H_{13}N_2]^+$= 137.12 Da, Found $[M + 1]^+$137.14 Da.

Synthesis of 1-isopentyl-1H-imidazole (IV)

Imidazole (1.0 g, 14.7 mmol) and KOH (1.2 g, 22 mmol) in 25 ml of DMSO stirred for 30 min followed by addition benzyl bromide (2.2 g, 14.7 mmol) and stirred for 5 h at room temperature. Product was isolated by following the same method of III. Yield: 88.5%. FT-IR (ATR cm^{-1}) 3089, 2935 (C–H $_{alip}$ str), 1462 (C–C str), 1382 (C–H ben), 1282 (C–N str), 877, 775 (C–H ben). UV–Vis (λ_{max} nm). 252.3, 234.6. MS (*m/z*): Predicted $[M + 1]^+$, $[C_{14}H_{11}N_2]^+$= 189.13 Da, Found $[M + 1]^+$189.11 Da.

*Synthesis of 1,2-bis(3-benzyl-2,3-dihydro-1H-benzo[*d*]imidazol-1-yl)ethane bromide salt (L1)*

A mixture of **I** (1.0 g, 6.25 mmol) and 1, 2-dibromoethane (5 ml, 57.7 mmol) refluxed (at 90 °C) in 1,4-dioxane for 18 h. Yellowish product was settled down, washed with petroleum ether. Yields: 77%. FTIR (ATR cm^{-1}): 2955, 2918 (C–H str), 1481, 1444 (C–C str), 1211, 1171 (C–N str), 739, 652 (C–H bend). ^{1}*H* NMR (400 MHz DMSO–d_6, δppm), 3.03 (s, 4H, 2×CH_2), 5.61 (s, 4H, 2 × *N*–CH_2), 6.62 (m, 4H, Ar-H), 6.91 (m, 4H, Ar-H), 7.40 (m, 10H, Ar-H), 9.11 (s, 2H, NCHN). ^{13}C NMR (110 MHz, DMSO–d_6, δppm), 49.4 (2C, N–CH_2), 77.6 (4C, Ar-C), 110.4 (4C, Ar-C), 120.0 (2C, Ar-C), 126.3 (4C, Ar-C), 127.6 (4C, Ar-C), 128.7 (2C, Ar-C-CH_2), 128.9 (4C, N–CH_2), 144.8 (2C, NCN). UV–Vis (λ_{max} nm): 261.7, 217.9. Anal. Calc. for $C_{30}H_{30}Br_2N_4$: C, 59.42; H, 4.99; N, 9.24. Found: C, 59.73, H, 4.89; N, 9.29.

Synthesis of 1,2-bis(3-benzyl-2,3-dihydro-1H-imidazol-1-yl)ethane bromide salt (L2)

A mixture of **II** (1.0 g, 6.33 mmol) and 1, 2-dibromoethane (5 ml, 57.7 mmol) was reacted by following the same procedure of **L1**. Yields: 63%. FT-IR (ATR cm^{-1}): 3047 (C $_{arom}$-H str), 2999, 2864 (C_{aliph}-H str), 1215, 1157 (C–N str), 1583 (*C = C* str), 1496, 1425 (C–H bend). ^{1}*H* NMR (400 MHz DMSO–d_6, δppm), 2.52 (s, 4H, 2×CH_2), 4.73 (s, 4H, 2 × *N*–CH_2), 5.50 (s, 4H), 7.51 (m, 10H, Ar-H), 9.42 (s, 2H, NCHN).^{13}C NMR (110 MHz, DMSO–d_6, δppm), 38.2 (2C, N–CH_2), 48.9 (2C, N–CH_2), 122.9 (4C, N–CH_2), 129.3 (2C, Ar-C), 134.9 (4C, Ar-C), 136.8 (2C, Ar-C-CH_2), 144.7 (2C, NCN). UV–Vis (λ_{max} nm): 247.5, 219.7. Anal. Calc. for $C_{22}H_{26}Br_2N_4$: C, 52.19; H, 5.18; N, 11.07. Found: C, 52.55; H, 5.27; N, 10.93.

*Synthesis of 1,2-bis(3-isopentyl-2,3-dihydro-1H-benzo[*d*]imidazol-1-yl) ethane bromide salt (L3)*

A mixture of **III** (1 g, 5.32 mmol) and 1, 2-dibromoethane (5 ml, 57.7 mmol) processed by the same procedure of **L1**. Yield: 65%. FTIR (ATR cm^{-1}), 2961 (C–H str), 1480, 1400 (C–C str), 829, 747 (C–H ben). ^{1}*H* NMR (400 MHz, DMSO–d_6, δppm), 0.92 (d, *J* = 4.0 Hz, 12H, 4×CH_3), 1.49 (q, 4H, 2×CH_2), 1.69 (m, 2H, 2×CH), 2.50 (s, 4H, 2×CH_2), 4.43 (t, 4H, 2 × *N*–CH_2), 7.60 (m, 4H, Ar-H), 7.67, 7.84, 8.09 (m, 4H, Ar-H), 10.07 (s, NCHN). UV–Vis (λ_{max}, nm): 276.3, 270.0. Anal. Calc. for $C_{26}H_{38}Br_2N_4$: C, 55.13; H, 6.76; N, 9.89. Found: C, 55.53; H, 6.84; N, 9.76.

2.1.8. Synthesis of 1,3-bis(3-isopentyl-2,3-dihydro-1H-imidazol-1-yl)propane, bromide salt (L4)

Mixture of **IV** (1.5 g, 10.86 mmol) and 1, 2-dibromoethane (5.5 ml, 63.5 mmol) reacted by following similar protocols of **L1**. Yields: 63%. FTIR (ATR cm^{-1}): 2958, 2872 (C–H str), 1564 (*C = C* str), 756 (C–H bend). ^1H NMR (400 MHz DMSO–d_6, δppm), 0.91 (d, J = 4.00 Hz, 12H, 4×CH_3), 1.52 (q, 4H, 2×CH_2), 1.81 (m, 2H, 2×CH), 4.73 (t, 8H, 4 × *N*–CH_2), 7.70 (s, 4H), 9.3 (s, 2H, NCHN). UV–Vis (λ_{max}, nm): 270.0, 219.1. Anal. Calc. for $C_{19}H_{36}Br_2N_4$: C, 47.51; H, 7.55; N, 11.66. Found: C, 47.94; H, 7.63; N, 11.51.

Synthesis of 3,3′-(ethane-1,2-diyl)bis(1-benzyl-1H-benzo[d]imidazole-2(3H)-selenone) (C1)

A mixture of **L1** (1.0 g, 1.7 mmol), K_2CO_3 (0.47 g, 3.4 mmol) and selenium powder (0.27 g, 3.5 mmol) was refluxed at 110 °C for 8 h in water. A blackish thick material was found attached with magnet bar and on the walls of the flask. Hot mixture was filtered through Whatmann filter paper and residue was left for drying. After drying the material was solubilized in DCM and again filtered through celite column and obtained crystal clear filtrate. This filtrate was placed in fumehood for overnight evaporation.Yield:62%. FTIR (ATR cm^{-1}): 3177, 3156 (C_{arom}-H str), 2955 (C_{alip}-H str), 1669 (*C = C* str), 1494, 1479 (C–C str), 1076, 1028 (C–H bend). ^1H NMR (400 MHz $CDCl_3$, δppm), 3.03 (s, 4H, 2×CH_2), 5.51 (s, 4H, 2×CH_2), 7.11 (m, 18H, Ar-H).^{13}C NMR (110 MHz, $CDCl_3$, δppm), 47.8 (2C, N–CH_2), 50.1 (2C, N–CH_2), 107.7 (4C, Ar-C), 111.6 (4C, Ar-C), 123.9 (6C, Ar-C), 127.6 (4C, Ar-C), 128.6 (4C, N–CH_2), 134.6 (2C, Ar-C-CH_2), 154.4 (2C, NCNSe). UV–Vis (λ_{max}, nm): 286.12, 277.61. Anal. Calc. for $C_{30}H_{26}N_4Se_2$: C, 60.01; H, 4.36; N, 9.33. Found: C, 60.38; H, 4.41; N, 9.28. MS (*m/z*, Da): [M-1] $^+$, $[C_{30}H_{25}N_4Se_2]^+$, Predicted = 601.05, Found = 601.18.

Synthesis of 3, 3′-(ethane-1, 2-diyl)bis(1-benzyl-1H-imidazole-2(3H)-selenone) (C2)

A mixture of **L2** (1 g, 1.98 mmol), K_2CO_3 (0.52 g, 3.99 mmol) and selenium powder (0.50 g, 6.2 mmol) was refluxed at 110 °C for 8 h. Yield: 51.8%. FTIR (ATR cm^{-1}): 2925 (C–H str), 1654 (*C = C* str), 1484 (C–C str), 1073 (C–H bend). ^1H NMR (400 MHz, $CDCl_3$, δppm), 1.12 (s, 4H, 2×CH_2), 2.53 (s, 4H, 2 × *N*–CH_2), 4.01 (s, 4H), 7.30 (m, 10H, Ar-H), ^{13}C NMR (110 MHz, $CDCl_3$, δppm), 39.6 (2C,CH_2), 48.9 (2C, N–CH_2), 123.6 (4C, N–CH_2), 129.4 (6C, Ar-C), 134.9 (4C, Ar-C), 137.2 (2C, Ar-C-CH_2), 154.3 (NCNSe). UV–Vis (λ_{max}, nm): 283.5, 275.21. Anal. Calc. for $C_{22}H_{22}N_4Se_2$: C, 52.81; H, 4.43; N, 11.20. Found: C, 53.05; H, 4.55; N, 11.09. MS (*m/z*, Da): [*M* + 1] $^+$, $[C_{22}H_{23}N_4Se_2]^+$, Predicted = 501.02, Found = 501.028,

Synthesis of 3,3′-(ethane-1,2-diyl)bis(1-isopentyl-1H-benzo[d]imidazole-2(3H)-selenone) (C3)

A mixture of **L3** (1.0 g, 1.78 mmol), K_2CO_3 (0.52 g, 3.89 mmol) and selenium powder (0.50 g, 6.2 mmol) was refluxed at 110 °C for 8 h by following the same procedure of C1. Yield: 46.3%. FT-IR (ATR cm^{-1}): 2956 (C–H str), 1656 (C=Cstr), 1481 (C–C str), 1259 (C–N str), 738, 651 (C–H ben). ^1H NMR (400 MHz, $CDCl_3$, δppm), 1.12 (d, J = 5.00 MHz 12H, 4×CH_3), 1.51 (q, 4H, 2×CH_2), 1.63 (m, 2H, 2×CH), 4.42 (t, 4H, 2 × *N*–CH_2), 4.95 (s, 4H, 2×CH_2), 7.25 (m, 4H, Ar-H), 7.5 (m, 4H, Ar-H). UV–Vis (λ_{max}, nm): 278.1, 272.0. Anal. Calc. for $C_{26}H_{34}N_4Se_2$: C, 55.71; H, 6.11; N, 10.00. Found: C, 55.97; H, 6.27; N, 10.08. MS (*m/z*, Da): $[M + 1]^+$, $[C_{26}H_{35}N_4Se_2]^+$, Predicted = 561.11, Found = 561.15.

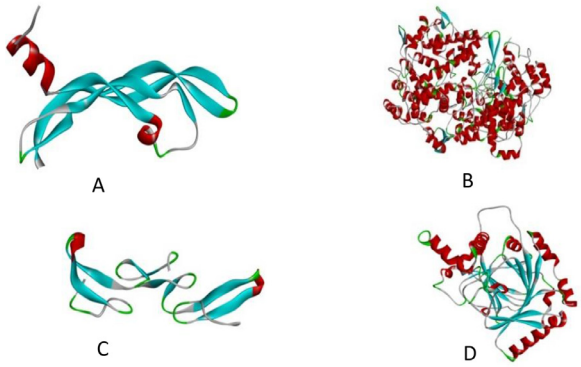

Fig. 1. A: VEGFA protein from RCSB protein data bank (4KZN), B: COX1 protein from RCSB protein data bank (1EQH), C: EGF protein from RCSB protein data bank (1JL9), D: HIFprotein from RCSB protein data bank (1YCI).

Synthesis of 3,3′-(propane-1,3-diyl)bis(1-isopentyl-1H-imidazole-2(3H)-selenone) (C4)

A mixture of **L4** (1.0 g, 2.12 mmol), K_2CO_3 (0.58 g, 4.25 mmol) and selenium powder (0.35 g, 5.0 mmol) was refluxed at 110 °C for 8 h by following the procedure of C1. Yield: 68.7%. FT-IR(ATR cm^{-1}): 2956, 2870 (C–H str), 1643 (*C = C* str), 1456 (C–C str), 1284 (C–N str), 970 (C–H bend). ^1H NMR (400 MHz, $CDCl_3$, δppm), 0.99 (d, J = 5.18 Hz, 12H, 4×CH_3), 1.52 (q, 4H, 2×CH_2), 1.62 (m, 2H, 2×CH), 1.75 (m, 2H, 1×CH_2), 3.91 (t, 8H, 4 × *N*–CH_2), 7.52 (s, 4H). UV–Vis (λ_{max}, nm): 277.3, 271.2. Anal. Calc. for $C_{19}H_{32}N_4Se_2$: C, 48.10; H, 6.80; N, 11.81. Found: C, 48.44; H, 6.93; N, 11.73. MS (*m/z*, Da): [M-1]$^+$, $[C_{19}H_{32}N_4Se_2]^+$, Predicted = 474.11, Found = 474.21.

Molecular docking of compound C_1–C_4

Protein preparation

For molecular docking of compounds C_1–C_4 with selected protein targets, Molecular graphics laboratory(MGL) tools were downloaded from http://mgltools.scripps.edu, Python language was downloaded from www.python.com and AutoDock4.2 was downloaded from http://autodock.scripps.edu, BioVia draw was downloaded from http://accelrys.com, Discovery studio visualizer 2017 downloaded from http://accelrys.com and Chem3D was downloaded from https://acms.ucsd.edu.The three dimensional crystal structure of anticancer targets VEGFA with PDB ID: 4KZN, COX1 with PDB ID: 1EQH, EGF with PDB ID: 1JL9, HIF with PDB ID: 1YCI were selected and downloaded from Protein Data Bank (www.rvcsb.org/pdb) (**Fig. 1**) [12]. The complexes bound to the receptor-molecule, all the non-essential watermolecules and heteroatoms were deleted and ultimately hydrogen atoms were added to the target receptor molecule using Argus Lab.

Ligand preparation

For the computational targets four synthetic active compounds (available with identified structure of ligands from crystallography) were used from Pubchem to make sdf format and converted to PDB format using Pymol which was further used for docking studies.

The starting structures of the proteins were prepared using AutoDock tools. Water molecule was deleted, polar hydrogen and Kollman charges were added to the protein starting structure.Grid box was set with the size of 126×126×126 Å with the grid spacing of 0.375 Å at the binding site. The starting structure for all the ligands namely 5 s, 6 s, C2 and C4 constructed using BioVia draw. 5FU was selected as positive control. Their structures were

provided from Pubchemwebsite Gasteiger charges were assigned into optimized ligand using Autodock Tools. 100 docking runs were conducted with mutation rate of 0.02 and crossover rate of 0.8. The population size was set to use 250 randomly placed individual. Lamarckian Genetic algorithm was used as the searching algorithm with a translational step of 0.2 Å, a quaternion step of 5 Å and a torsion step of 5 Å.

Stability assay

The stability of synthesized compounds was studied through spectral studies by monitoring spectral behavior for specific period through UV-Visible spectroscopy. The studied compounds were solubilized in minimum amount of Acetonitrile diluted further to 10^{-4} M with PBS and their UV–Vis spectra were monitored for 0, 16, 24, 48, 96 h, respectively, by following the protocol of [13].

Lipophilicity assay

Lipophilic values of synthesized compounds in terms of log P was measured through ability of prinpartitioning of studied compound between octanol and aqueous layers. UV–vis spectroscopy based method was used to estimate the concentration of studied compounds in each layer/phase. Briefly, 0.5 mg of each compound (L1-L4) in distilled water and (C_1–C_4) in Acetonitrile respectively and Log P value was measured through logarithm of ratio of concentration in octanol layer to aqueous layer by formula (Log P=Log ([org]/[Aq]).

Interaction with BSA

UV-visible spectrophotometric method was used for interaction study of increasing concentration of synthesized molecules with constant concentration(0.01 mM) of BSA by following the protocol of [14]. Shift in spectrum of BSA-drug solutions was measured as an indication of drug-BSA binding compared to both BSA and compound solutions individually. FTIR-ATR based study was also conducted to investigated the mode of affinity among synthesized compounds and protiens [15].

Cytotoxicity

Cytotoxicity of synthesized compounds against three cancer strains was measured through MTT assay by following the method of [16]. The amount of formazan product is directly proportional to number of living cells present. Synthesized compounds C1-C4 and L1-L4 were prepared for a series dilution (10–0.001 µg mL^{-1}) in Methanol and water respectively and standard drugs 5-Florourouracil, oxaliplatin and cisplatin (1–0.0001 µg mL^{-1}) in methanol. Human cancer cell lines MCF-7 (1000 cell/well), lung cancer cell A549 (1000 cell/well) and breast cancer cell line HCT-116 (1000 cell/well) were cultured in DMEM medium (Dubecco's modified Eagle medium) in the presence of 5% CO_2 continuous aeration at 37 °C in 96 well plate with 100 µL medium and incubated for 24 h. After 24 h, replaced the DMEM with freshly prepared DMEM with 10 µL of each concentration of samples were added. For the accuracy of the experiment, treatments were performed in triplicate. Control was set as to grow cell line without drug treatment which holds only living cells in well and triplicate of blank DMEM was also adjusted on 96 well plates. After 48 h incubation, 20µL of MTT dye (5 mg/ml in PBS) was added in each well and allowed to incubate at 37 °C for four hours. Contents of wells were removed and frozen product was solubilized in 100µL DMSO hence, the purple color appeared. The absorbance of each well was measured on Biobase multiplate reader through Gen 2.0 software at 570 nm and% viability of cells were calculated through following formula

$$\%\ cell\ viability = \frac{ODsmp}{ODcontrol} \times 100$$

OD is the optical density measured at 570 nm.

Results and discussions

Synthesis

Synthesis of precursors (**I-IV**), bis-azolium molten salts (**L_1-L_4**) and their selenium adducts (**C_1–C_4**) was accomplished through procedures of [17] with minor modifications that described in *Scheme 1*. Synthesis of precursors (**I-IV**) was achieved in first step through N-alkylation that involved deprotonation from terminal Nitrogen of azolium (imidazole and benzimidazole) moiety with the aid of strong base (KOH) followed by alkylation (R_1) at N_1 with selected alkyl halides. In the second step, alkylation on second Nitrogen (N_2) of precursors was made by refluxing precursor (**I-IV**) individually with 1,2-dibromoethane in 1,4-dioxan for 24 h which yields Ionic liquids **L_1-L_4** with bromide as counter ion and became readily water soluble due to their ionic nature. These ILs L_1-L_4 were refluxed with potassium carbonate and selenium powder in water medium for 8 h by following simple procedure of [18] which yields selenium adducts (**C_1–C_4**). The replacement of organic solvent with water for sysnthsis of selenium compounds was termed as green synthesis [19]. A sticky blackish fluid insoluble in water attached with magnet bar as well as walls of the flask, which was later separated, dried and dissolved in chloroform and passed through celite column which produced light yellowish fluid product.

Characterization

The imidazolium and benizimidazolium based precursors (**I-IV**) were confirmed through Ultra high pressure Liquid chromatography (UHPLC) hyphenated with spectroscopy (PDA) and mass spectrometry (ESI-MS). Synthesized molten salts (**L_1-L_4**) were characterized by spectroscopic techniques (UV-spectrophotometer, FTIR), ^1H & ^{13}C NMR and mass spectrometry. The selenium adducts (**C_1–C_4**) were characterized through distinguished behavior observed in FTIR, ^1H & ^{13}C NMR as well as confirmed through mass spectrometry.

UHPLC-PDA/MS

Syntheses of precursors **I-IV** were assured through UHPLC-PDA by measuring their retention time (RT) as well as UV-Visible spectra in comparison to azolium base. The purity of precursors was also assured through single peak as well their 3D spectra thorugh Photodiod array detector (PDA). When precursor **I** was analyzed through UHPLC-PDA, a prominent peak at RT 2.388 min was observed which was different from benzimidazole (RT: 2.154 min) confirming the different chemical nature of precursor **I** from benzimidazole. Additionally, Precursor **I** showed UV-visible spectrum with absorption maxima at 212.0 and 248.8 nm which was different from its reactant. The synthesis of **I** was further assured through mass spectrometry which recorded major peak at 207.21 for their parent ion $[M\text{-}1]^+$**Fig. 2.** Precursor **II** showed RT 2.55 min having unique UV-visible spectrum different from imidazole which indicated the difference in chemical nature as an indication of substitution at imidazole for precursor **II** and detailed spectra are provided in supplemantry data **Fig. S1**. UHPLC-ESI-MS spectrum further confirmed the successful synthesis of Precursor **II** by showing prominent parent ion peak $[M + 1]^+$ for substituted imidazole Pre-

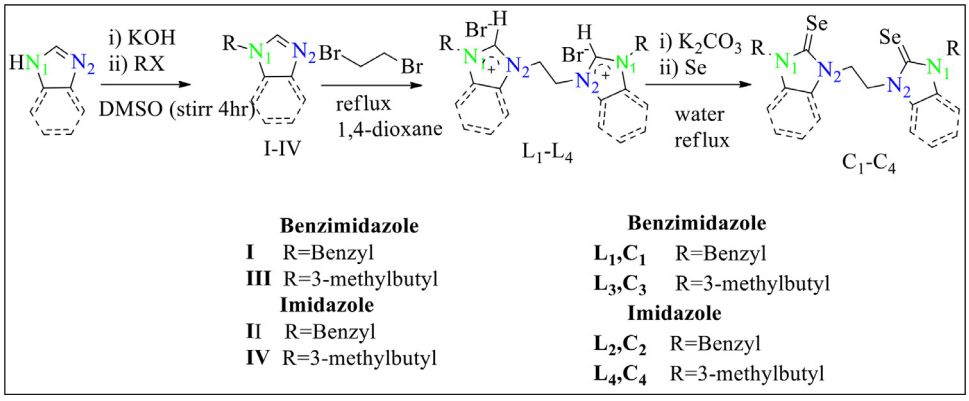

Scheme 1. Synthesis of precursors (**I-IV**), salts (**L_1-L_4**), selenium adducts (**C_1–C_4**).

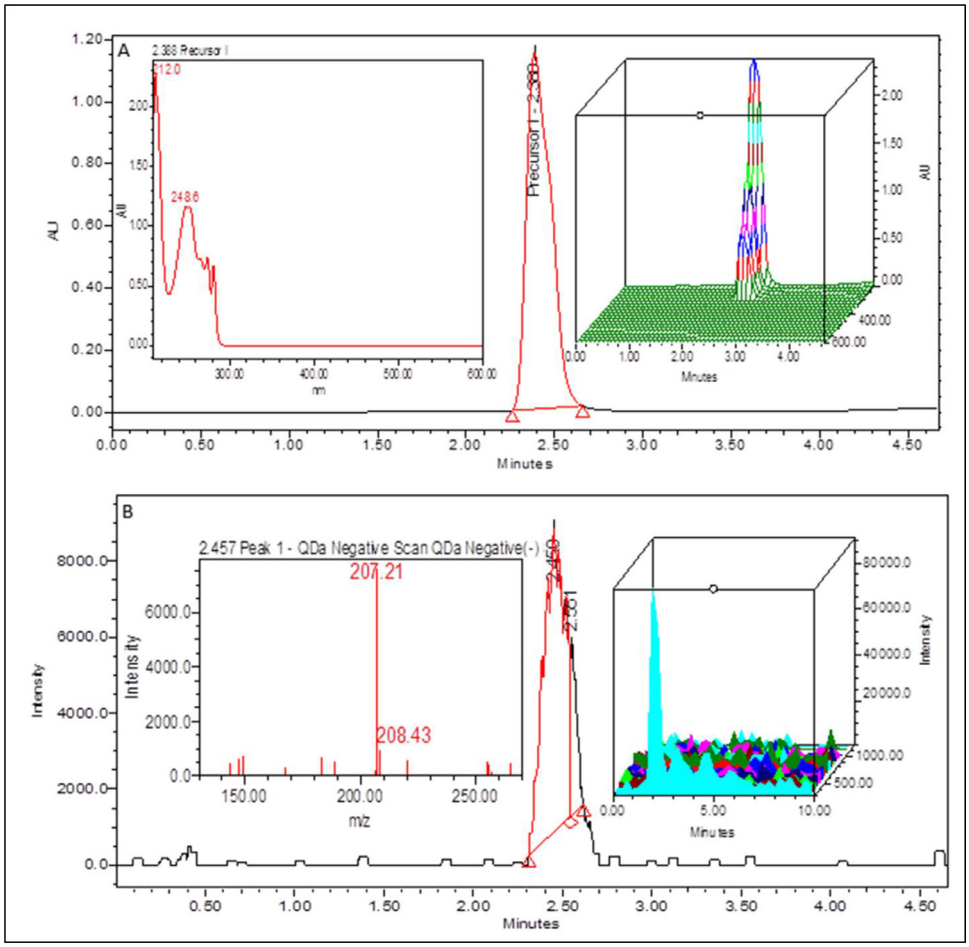

Fig. 2. A) UHPLC-PDA (UV–Vis.) chromatogram and spectrum at specific peak RT 2.38 min of precursor **I,** B) UHPLC-QDa (ESI-MS) at RT 2.45 min at negative mode with spectrum and 3D imaging of precursor **I**.

cursor **II** coincide with its theoretical expected mass supplemantry data **Fig.S1**. The Preucrsors **III & IV** were also measured through UHPLC-PDA/ESI-MS at both positive and negative ion mode at varied capillary voltage (9–15 V) and observed their molecular ion peaks at 189.20 and 137.21 Da for Precursor **III &IV**, respectively which is in accordance with parent ion peak of mass spectra of **III & IV** predicted through computational software (ChemDrawUlta 12.0) and also measured for their UHPLC-PDA chromatograms and spectra that confirmed the purity as well as successful synthesis of Precursors, chromatrographic results are provided in supplemantry data **Fig. S1-S2**.

When ILs (**L_1-L_4**) studied through UHPLC-PDA, a far difference in absorption spectra from than that of respective precursors **I-IV** and shift in retention time was observed, results are provided in supplemantry data **Fig. S3-S6**. This difference in absorption spectra could be attributed to formation of molten salts by combining precursor's **I-IV**. However, very minor difference in absorption spectra of selenium adducts (**C_1–C_4**) was observed in comparison to their respective ligands, supplemantry data **Fig.S6a**. This minimal difference among the spectral behavior could be due to minor modificaton of molecular structure of binuclear salts **L_1-L_4** and addition of unsaturation by replacing proton of carbene carbon through el-

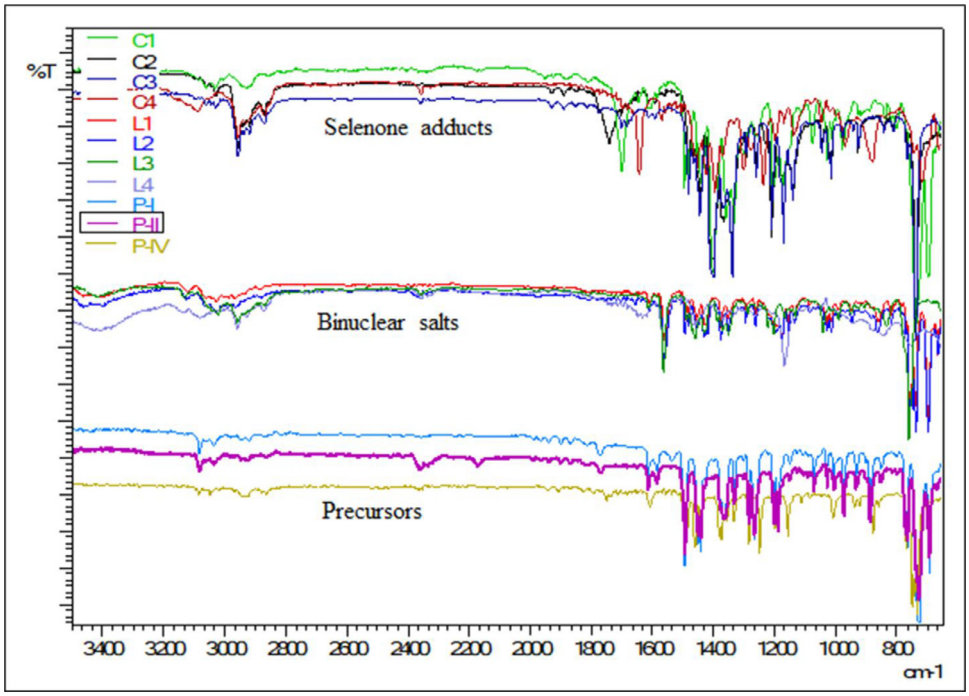

Fig. 3. overlay FTIR spectra of precursors **I-IV**, binuclear salts $\mathbf{L_1}$-$\mathbf{L_4}$ and selenone compounds $\mathbf{C_1}$–$\mathbf{C_4}$ from bottom to top respectively.

emental selenium. Selenium adducts were further assured through mass spectrometery (HRMS) which confirmed the successful conversion of ILs into respective adducts and results are provided in supplemantry data **Fig.S19-S22.**

FTIR spectroscopy

FTIR spectroscopy was applied for the investigation of Precursors (**I-IV**) and their conversions into ILs ($\mathbf{L_1}$-$\mathbf{L_4}$) through peculiar behavior observed in spectra, Fig. 3. An intense peak pattern in the range of 800–650 cm^{-1} of =*C*–H bending vibrations was observed in all spectra of precursors and salts irrespective of the nature of substitution. A sharp peak pattern of aromatic *C* = *C* stretching in the region of 1650–1500 cm^{-1} was observed for **I** & **III** but weak for **II** & **IV** which differentiates imidazolium and benzimidazolium precursors [20]. Similarly, an intense peak at 1300–1450 cm^{-1} for precursor **I** & **III** and weak for **II** & **IV** marked the difference among *N*-alkylated benzimidazolium and *N*-alkylated imidazolium precursors. A prominent peak region (3250–3140 cm^{-1}) could be attributed to substitution at N_1 position through replacement of proton with alkyl and aryl groups [21]. The successful conversion of precursors into ILs $\mathbf{L_1}$-$\mathbf{L_4}$ was marked through shift in spectral behavior from their precursors, Fig. 3. The distinguished spectral patterns appeared in spectra of bis-azolium salts ($\mathbf{L_1}$-$\mathbf{L_4}$) at around 2890–3010 cm^{-1} (C–H_{aliph}) due to attachment of alkyl linker that differentiates ligands from the respective precursors.

The conversion of ligands into selenium adducts ($\mathbf{C_1}$–$\mathbf{C_4}$) were measured through changes in FTIR spectra in comparison to respective ILs ($\mathbf{L_1}$-$\mathbf{L_4}$) by highlighting typical changes appeared in comparative spectra Fig. 3. Some distinguished pattern of FTIR spectra of Se-NHC adducts comparing to their azolium salts at 1450–1100 cm^{-1} was observed that could be linked with vibrational frequency of carbon selenium (*C*=Se) bonds. The same behavior was confirmed through literature showing vibrational frequency at 1222 cm^{-1} for *C*=Se of imidazolium adducts [19].The prominent region at 1560–1500 cm^{-1} for molten salts $\mathbf{L_1}$-$\mathbf{L_4}$ was suppressed in selenium adducts ($\mathbf{C_1}$–$\mathbf{C_4}$) an indication of successful conversion of ligands into adducts. The similar trend was also observed by Iqbal, Haque, Ng, Hassan, Majid and Razali [19] who reported the suppression of this region upon incorporation of elemental selenium in organic framework of imidazolium salts. The comparable characteristic pattern was observed by [18] for mononuclear selenium adducts showing suppression in stretching frequency of this functional group, **Fig. 4**.

NMR spectroscopy

Successful synthesis of salts ($\mathbf{L_1}$-$\mathbf{L_4}$) and compounds ($\mathbf{C_1}$–$\mathbf{C_4}$) were also confirmed through ^{1}H & ^{13}C NMR spectroscopy, and detailed NMR description is given in experimental section. Resonance of aromatic proton of imidazolium and benzimidazolium salts ($\mathbf{L_1}$-$\mathbf{L_4}$) was observed in 7.0 - 8.3 ppm, which is in line agreement with previous reports showed similar region of resonance for aromatic proton of azolium salts [22]. However, the peculiar behavior observed for bis-azolium salts ($\mathbf{L_1}$-$\mathbf{L_4}$) was the appearance of characteristic singlet resonance peak at aroud 9.0–12.0 ppm appeared in ^{1}H NMR spectra that diminished with incorporation of elemental selenium in the organic framework of salts, detailed spectra are provided in supplemantry data **Fig S7-S13.** The appearance of this characteristic peak in salts $\mathbf{L_1}$-$\mathbf{L_4}$ at 9.1, 9.4, 10.0 and 9.3 ppm respectively is associated with resonance of carbene proton (NCHN) supplemantry data **Fig S7-S10**. These observations were consistent with literature which showed presence of carbene proton in this region [23,24]. This peculiar peak of carbene proton disappeared in selenium adducts $\mathbf{C_1}$–$\mathbf{C_4}$ due to replacement of carbene proton with elemental selenium, an indication of successful conversion of carbene salts into their respective compounds ($\mathbf{C_1}$–$\mathbf{C_4}$) [25]. The successful synthesis of salts ($\mathbf{L_1}$-$\mathbf{L_4}$) was also confirmed through ^{13}C NMR spectra where a peculiar peak at 140–150 ppm is associated with carbene carbon (NCHN), supplemantry data **Fig S14-S17**. The similar observations were reported with chemical shift (^{13}C, ppm) at 143.0, 142.6, 143.0 [22] and 144.7, 142.1 [26] for carbene carbon (NCHN) of azolium salts. Interestingly this characteristic peak of carbene carbon shifted to low field (152.5–160.5 ppm) when proton of carbene carbon is replaced with elemental selenium, described in **Fig. 4**. The other detailed NMR description is

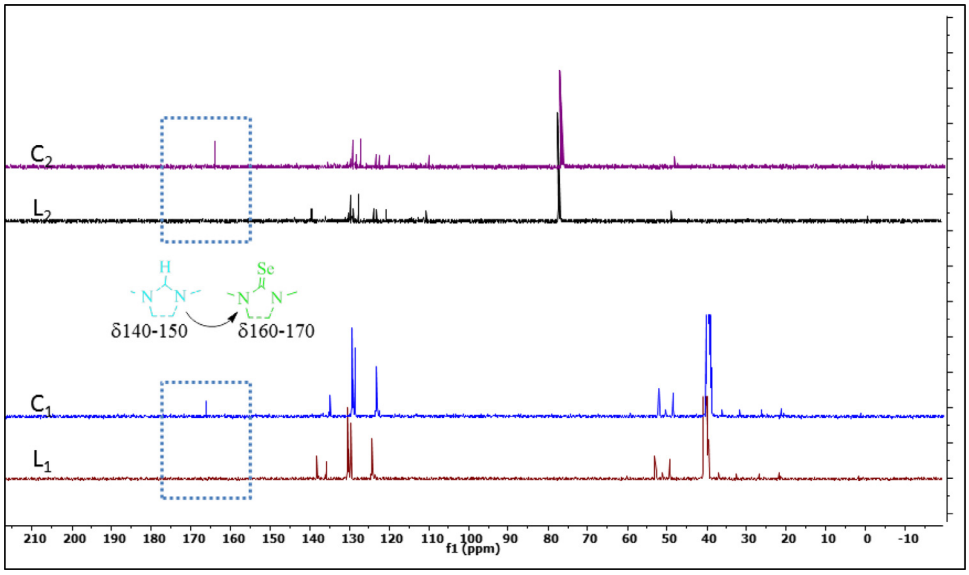

Fig. 4. overlay spectra of ^{13}C NMR of ligands L1-L2 and compounds C1-C2.

Table 1
Log *P* values of compounds $\mathbf{C_1}$–$\mathbf{C_4}$ in aqueous-octanol system.

Compound	C_o (mg L^{-1})	C_w (mg L^{-1})	Log P
$\mathbf{C_1}$	9.32	0.68	1.13
$\mathbf{C_2}$	8.45	1.55	0.74
$\mathbf{C_3}$	9.57	0.43	1.34
$\mathbf{C_4}$	8.59	1.31	0.82

provided in the experimental section and spectra are provided in supplementary files **Fig S7-S17**.

Stability in solution

The stability of compounds ($\mathbf{C_1}$–$\mathbf{C_4}$) were studied through UV-Visible spectroscopy in solution form. The studied compouds 0.2 g dissolved individually in Acetonitrile (ACN) and diluted with PBS solution 0.02 g/mL. The time dependent (16, 24, 36, 48, 96 h) UV–Vis spectra of solutions exhibit no apparent spectral changes over the studied time course given in supplemantry data **Fig.S22**. This repetitive behavior of compounds with time course showed that compounds are stable at ambient temperature in solution form for studied time period. These results were further confirmed through HPLC-PDA which showed repetitive chromatographic behavior over studied time course, which showed that studied compounds are stable at physiological conditions for studied time course.

Lipophilicity determination

Hydrophilicity/lipophilicity is very important parameter specified by Lipinski's rule for drug development, it exhibits the ability of drug to cross biological membrane and determin druggability. The lipophilic character of selenium adducts $\mathbf{C_1}$–$\mathbf{C_4}$ was measured through flask shake method and the values are presented in $P_{o/w}$ given in **Table 1**. The lipophilic values of compound $\mathbf{C_1}$–$\mathbf{C_4}$ indicate that these compounds are sufficiently lipophilic to satisfy the general lipophilic requirement of drug. Among the studied compounds $\mathbf{C_1}$ and $\mathbf{C_3}$ are more lipophlic than $\mathbf{C_2}$ and $\mathbf{C_4}$ which could be due to nature of substituent at azolium moiety. The previous reports suggest that cell membrane permeability and cytotoxicity of compounds is very much dependent upon lipophilicity of compounds [13]

Interaction studies with BSA (Bovine serum albumin)

Human serum albumins (HSA) are principle proteins responsible for binding and carrier of diverse drug entities. However, BSA (bovine serum albumin) is the most studied conjugate protein due to high similarities with HSA that mimics in reactivity to study various metal–based complexes for their potential selective targeting to HSA [27]. A large number of metals, be it Pt^{2+}, Cu^{2+}, Zn^{2+}, Ni^{2+} and Co^{2+} complexes have been investigated for their interaction with BSA in relationship to their bioactivity. However selenium based NHC adducts were not studied for their potential interaction with albumins. Therefore, organ-selenium adducts ($\mathbf{C_1}$–$\mathbf{C_4}$) were studied for their intrinsic binding affinity with albumin proteins in terms of binding constant K_b through spectroscopic titrations.

The absorption spectrum of BSA showed characteristic absorption maximum at 280 nm due to aromatic amino acid residues. On sequential addition of incremental aliquots of drug $\mathbf{C_1}$ (0.647–2.59 μM) to a fixed concentration of BSA, a sharp increase in absorption intensity with slight shift in absorption pattern from 280 nm to 274 nm was observed, supplemantry data **Fig.S23** The shift in absorption pattern could be linked to binding of drug with studied proteins and furthermore, increase in intensity with respective increase in concentration of $\mathbf{C_1}$ was observed. The quantitative assessment of binding interactions of complex $\mathbf{C_1}$ with BSA ascertained the intrinsic binding (K_b $2 \times 10^5 \pm 0.06$) M^{-1}. The profound change in absorbance towards blue shift is an indication of formation of adducts of studied complexes with BSA [28] that showed concentration dependent response. In similar protocol compound $\mathbf{C_2}$–$\mathbf{C_4}$ were also investigated for their potential binding for BSA through intrinsic binding constants (Kb) with increasing concentrations of aliquots while concentration of BSA constant. The binding ability of studied compound is very much dependent on nature ofdrug that affects the binding strength with albumin proteins [29]. Interestingly, overall binding affinity of all drugs was far superior to reported literature for cisplatin ($K = 8.52 \times 10^2$ M^{-1}). Cisplatin is an FDA approved chemotherapeutic agent but notorious for nonselective in action [30].

The interaction of BSA was further investigated through FTIR spectroscopy based on the assessment of changes in amide bands of BSA upon interaction with $\mathbf{C_1}$. The most prominent bands appeared in the spectrum of BSA at 1750–1650 cm^{-1} and 1550–1500

Table 2
Binding constant values (K_b) and equation parameters of compound **C_1–C_4**.

Compound	Equation	Linear cofficient	K_b (M^{-1})
C_1	$Y = 0.025X + 0.362$	0.948	6.91×10^4
C_2	$Y = 0.387X + 0.016$	0.977	2.42×10^6
C_3	$Y = 0.032X + 0.596$	0.813	5.62×10^3
C_4	$Y = 0.283X + 0.031$	0.979	9.13×10^5

cm^{-1} could be attributed to $C = O$ streching and C–N streching of amide I and amide II of BSA respectively. Graphical results provided in supplemantry data **Fig.S24** showed a clear difference in spectrum of BSA-**C_1** from BSA with slight shift in frequency bands as well appearance of new bands that could be associated with interaction of selenium compounds with BSA. The slight shift in BSA spectra from 1740 to 1732 cm^{-1} could be due to engagement of amide I band with the drug because it is most vulnerable for the structual changes of protein. In the BSA-**C_1** spectra, appearnace of new bands with three disntint peaks in the region of 1250–750 cm^{-1} may be an indication of binding of drug with BSA and generated new function groups. Interstingly intensity of this region regularly changed with respective concentration of drug which indicates that interaction among them is concentration dependent phenomenon. The similar findings was also reported in literature when interaction of mimosine with BSA was studied through FTIR spectroscopy [14].

When compounds **C_2–C_4** were studied through UV-Visible spectroscopy for their binding affinity with BSA, no specific trends were observed as described in *Table 2*. Compounds C_1 & C_3 showed affinity for BSA molecules with K_b values 6.91×10^4 and 6.91×10^4 far better than Cisplatin 8.52×10^2 [31] but slightly lower than **C_2** & **C_4** having K_b 2.42×10^6 and 9.03×10^5 respectively.This change in affinity trends may be attributed to the lipophilic character which helps in intrinsic binding of drug with biological molecule. This fact was supported by Chen, Wang, Sun, Zhang, Sun, Sun, Shang and Luo [32] who claimed that lipophilic character may increase the effect on conformational changes in BSA that ultimately played a role in protein-drug binding phenomenon. Among the possible interaction forces, lipophilic interaction is considered as more prominent role in the intrinsic binding affinities with protein molecule [33]. Although no trend was reported among binding affinity of drug with BSA and bioactivity of drug but an interesting trend was observed in compounds **C_1–C_4** that compounds having lower Kb values showed more cytotoxicity.

Compounds C_1–C_4 titrated with BSA and a curve is drawn individually among 1/Conc. and Log of response factor. Equations of best fit curve is measured and Kb value is slop to intecept ratio

Hemolytic assay

Synthesized selenium compounds C_1–C_4 were studied for their hemolysis activity by measuring the destruction ability of compounds for RBCs through spectroscopic method and compared with possitive control Triton X. It was observed that all studied selenium compounds were found very least toxic thant possitve control Triton X, Fig. 5. The intra comparison of compounds for their hemolysis against RBCs showed that imidazolium based compounds (C_2 & C_4) were more inocuous for RBCs than that of benzimidazolium (C_1 & C_3). The overall hemolysis potential of compounds C_1–C_4 was found in the range of (09.8–18.6)% hemolysis which is in the safer range if used as drug. The lower hemolytic activity of selenium compounds (C_1–C_4) than Triton X showed that these compounds are almost safer and could proceed for further studies.

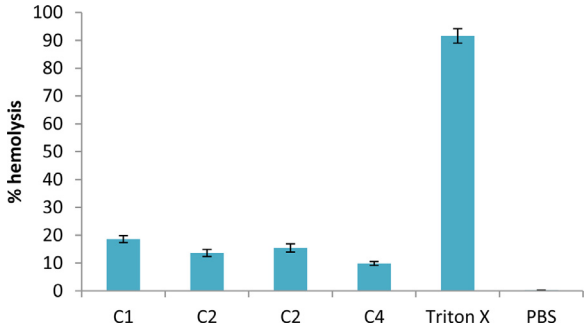

Fig. 5. % hemolysis of compound **C_1–C_4**, Triton X at concentration 0.1 mg mL^{-1} and PBS against humane RBCs.

Table 3
Inhibitory Concentrations (IC_{50}) of C1- C4.

Compound	IC_{50} (μg/mL)		
	MCF-7	HCT116	A549
C1	1.2768± 0.15	1.074± 0.08	1.3251± 0.05
C2	0.8691± 0.12	1.116± 0.09	0.9850± 0.08
C3	0.9813± 0.09	1.101± 0.14	0.9970± 0.12
C4	1.3787± 0.17	1.099± 0.13	0.9773± 0.17
5-FU	0.9978± 0.06	0.9981± 0.11	–
Oxaliplatin	–	–	0.808
Cisplatin	–	–	0.812

IC_{50} (μg/mL) values of compounds C1-C4, standard drug 5-flourouracil (5-FU), oxaliplatin and cisplatin for cancer cell lines Mcf-7, HCT116 and A549 was measured in triplicates and presented Mean ± SD.

Cytotoxicity

The synthesized compounds L_1-L_4 and C_1–C_4 were tested for their cytotoxicity against three cancer cell line, human colon cancer HCT 116, lung cancer A549 and breast cancer cell line MCF-7 through MTT assay. Reuslts of the studied compounds were compared with standard drugs 5-flourouracil(5-FU) and platin compounds cisplatin and oxiplatin and results are presented in **Fig. 6**. The ILs L_1-L_4 showed IC_{50} values in the range of 8.6–15.4 μg mL^{-1} for cancer cell line HCT-116 which seems very poor than standard drug 5-FU (0.9981±0.11 μg mL^{-1}). But cytotoxicity of these salts was surprisigly changed upon conversion to compounds C_1–C_4 which showed very good IC_{50} value in the range of (1.074–1.116 μg mL^{-1}) and very near to standard drug 5-FU. Then selenium compounds C_1–C_4 were further investigated for cancer cell line A459 where they showed exceptionally good cytotoxicity but slightly poor than standard drugs cisplatin and oxaliplatin, detailed results are described in **Fig. 6** and **Table 3**. The results showed that studied compounds showed concentration dependent response to inhibit the all cancerous cell lines which showed very good activity when compared with control. The most potent activity of compound C_1 (0.987± 0.05 μg mL^{-1}) was observed against A549 and C2 (0.8691 μg mL^{-1}) against MCF-7 which showed even better potential than standard drug 5-FU (0.9978± 0.06 μg mL^{-1}) while other compounds also showed good activity but slightly less than the standard drug.

Overall it was observed that selenium adducts C_1–C_4 are more potent than their binuclear salts L_1-L_4 which indicates the possible contribution of selenium center in the organic framwork of heterocyclic compound to exhibit bioactivity agaisnt cancer strain. The studied compounds C_1–C_4 showed better anticancer activity than reported mononuclear Se-NHC adducts [18] and similar in level in activity with silver complexes [23]. When anticancer potential of compounds was observed in correlation with lipophilicity of studied compouds, a very keen relationship was observed; which indi-

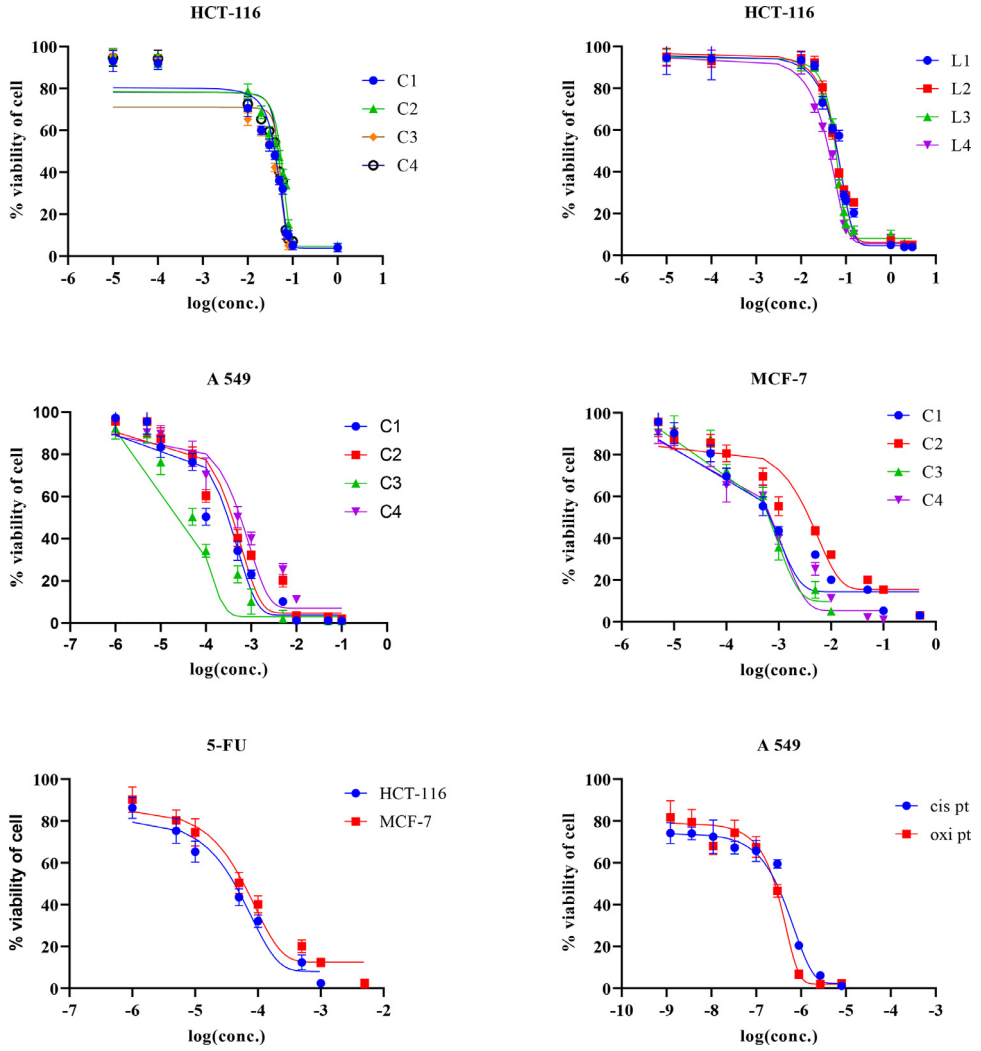

Fig. 6. *In vitro* anticancer activity of synthesized compounds C_1–C_4 and salts L_1-L_4 against cancer cell line HCT-116, A549 and MCF-7 thorugh MTT assay in comparison to standard drugs 5-Flourouracil (5-FU), Oxaliplatin (oxi pt) and cisplatin (*cis* pt). All the experiments were conducted in triplicate and presented in mean±SD.

cates that lipophilicty has direct effect on the bioactivity of compounds [34]. Similar observations were also reporeted in literature showing a sucessful correlation among lipophilicity and cytotoxicity of studied drugs [35].

Molecular docking

Angiogensis is a necessary factor for cancer growth, which ususally results by imbalancing of positive and negative angiogenic factors produced by cancer cell funtioning. Targeting these specific factors could be a selective anti-angiogensis approach which appeals the attention of medical scientists to investigate potential of drugs to hamper these factors. Among the growing factors in cancer cell, level of COX-1 (Cyclooxygenase-1), EGF(humanepidermal), VEGF-A(vascularendothelial, FactorA) and HIF (Hypoxia-inducible growth factor) have been found in direct correlation with tumorigensis. Therefore simulation studies for binding efficiency of active sites of selenium compounds C_1–C_4 with COX-1, EGF, VEGF-A and-HIF were studied through automated docking systems. The simulative potential of selenium compounds was measured through two parameters *i.e.* free binding energies as well as interaction binding constant (Ki) and results were compared with standard drug 5-Flourouracil (FU). The docked conformation of active sites of studied compounds with protein active factors COX-1, EGF, VEGF-A, HIF clearly demonstrate that there is numerous interaction potential of compounds was found with selected targets and results are summarized in Table 4.

Docking with COX1

The Interaction of selenium compounds with COX1 is shown in **Fig. 7** which revealed that free binding energy of compound C1,C3 & C4 are very lower than that of FU. Free binding energies of all selenium compounds except C_2 was lower than positive control FU for growing factor COX1 while C2 showed almost equal response to FU **Table 4**. This difference in free energy of compounds while interacting with COX1 could be linked with difference in bonding natures of active sites of compounds with protein target and defined the strength of bonding as well as free energy. Compound C2 showed C–H bonding with GLN461 bond length (BL) of 3.23 while C1 and C4 interacts with COX1 through C–H bonding with ASP135 having BL 3.17 and 3.01 respectively.C4 also showed some alkyl interaction with COX1 with ARG49, TRP323, ILE46, TYR130, LEU152, LYS46, VAL48, PRO153, CYS47, CYS36 and CYS41. Moreover, Compound C3 interacts with COX1 making pi sulfur bond with CYS36 and pi anion bond with GLU465 and pi sigma with LEU152. These differences in interaction sites for different compounds may affect the drug efficacy. Overall it was observed that aromatic

Table 4
Bindingenergy and inhibition constant of compounds C_1–C_4.

		COX1	EGF	VEGF	HIF
Binding energy (KJ mol^{-1})	C_1	−12.95	−7.56	−6.35	−10.12
	C_2	−5.15	−4.51	−4.99	−3.69
	C_3	−11.02	−6.89	−5.85	−7.57
	C_4	−10.09	−7.36	−6.24	−7.88
	5FU	−5.09	−4.97	−6.71	−5.26
Inhibition constant (μM)	C_1	3.2×10^4	2.90	3.31	3.8×10^4
	C_2	166.71	49	221.6	1.96
	C_3	3.9×10^3	8.96	19.40	5.6×10^5
	C_4	4.4×10^5	4	26.56	1.67
	5FU	187.11	227.34	12.12	138.96

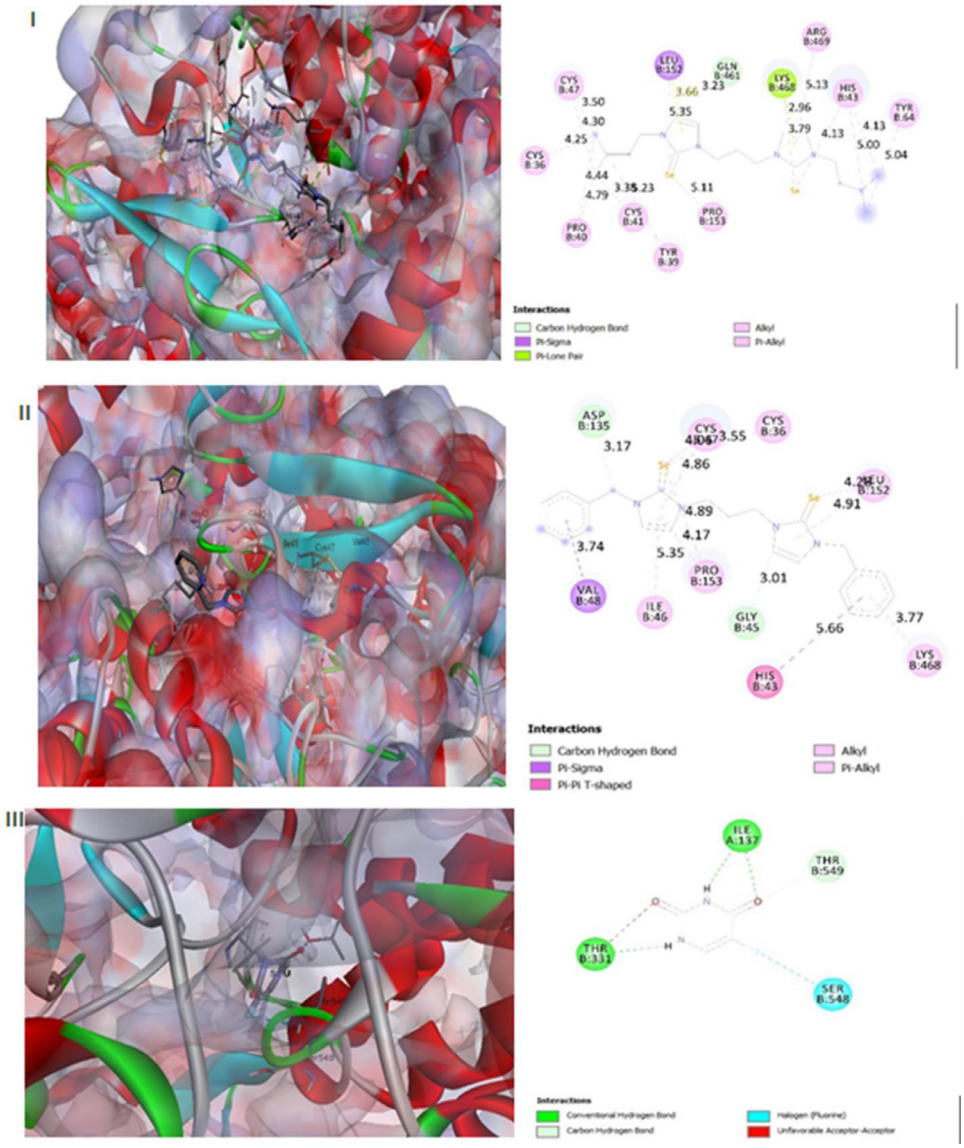

Fig. 7. Molecular docking of selenon compounds with protein target COX 1 with I) compunds C_1, II) Compound C_2, III) standard drug 5-FU.

groups helped more to lower the free binding energy while interacting with COX1. Since C2 has shown some pi sigma binding with LEU152 BL 5.35 while C4 has shown pi sigma binding with VAL48 BL 3.74 which make difference in binding energies of interaction of these compounds with targeted protein. In addition C4has shown pi-pi T shaped binding with HIS43 and few alkyl bindings with CYS67, CYS36, LEU152, PRO153, LEU46 and LYS468. This phenomenon's reason for stabilization of active pocket of COX after being in interaction with C1, C3 and C4 ended in less free binding energy than 5FU. 5FU has shown 3 H-bondings with LEU101, SER118 and GLN147 and showed free binding energy of −5.09 Kcal/mol. The compound C2 showed −5.15 Kcal/mol and other compounds C1, C3 and C4 showed-12.95, −11.02 and −10.09 Kcal/mol respectively.

Docking with EGF

The Interaction of selenium compounds with EGF is shown in supplemantry data **Fig. S25** which revealed that free binding energy of compound C1&C4 much lower than other competing compounds as well as from standard drug FU. Compound C4 has shown Pi lone pair with TYR37 and GLY18 BL of 2.96 and 2.91 respectively,Pi anion binding with ASP11 while C–H boding with CYS14 and ASP17. Ithas also demonstrated some alkyl bonds with LEU15, CYS6 and CYS20. Although 5FU involved 6 conventional hydrogen bonds through LEU8, CYS14, ASP11, PRO7, GLY12, TYR13 and CYS14 but compounds C1 and C3 contain 4 and 2 aromatic groups that are involvedin Pi binding which stabilized the active pocket more than FU and cause lower binding energy in them as compared to the positive control [36]. Moreover, C3 also showed C–H bonding with CYS31 and TYR37 and also Pi- alkyl bindings with ILE23, CYS33, TRP49, ALA30 and ILE38 from EGF which helps C3 to bind pocket and get stabilized more than 5FU [36]. On contrary Compound C2 demonstrated C–H bondings with CYS14 and ASP17 and few alkyl bondings with LEU8, CYS20, HIS16 and LEU15. Free binding energy of C2 was detected at −4.51 Kcal/mol while it has been −7.56 Kcal/ mol for C1. This significant difference maybe due to stability of the bonding pocket [36]. Although 5FU involves in 6 conventional hydrogen binds through LEU8, CYS14, ASP11, PRO7, GLY12, TYR13 and CYS14. But due to aromatic compound in structure of C1 as well as short bindings which happened in interaction with EGF, it stabilizes more than 5FU and C2, So it has more affinity towards EGF than other compounds.

Docking with VEGFA

The selenium compounds showed interaction with VEGFA as is shown in supplemantry data **Fig. S26**, but binding energy of all studied compounds was higher than standard drug FU. However among the selenium compounds,free binding energy of C1 is lower than which may be due to 4 aromatic rings in its structure that caused pi-pi T shaped bond [36]. On the other hand benzimidazolium compound C3 showed higher free energywhen interacts with VEGFA by making pi sulfur bond with MET78, and making pi sigma with ILE91. This compound contains 2 aromatic compounds so it needs to consume more energy to react with VEGFA compared with 6S or 5FU [37]. 5FU interacted 4hydrogen bonds with VEGFA via PHE47, PHE36, and ASP34 that made it to cause stronger affinity towards VEGFA than compound C1 & C3[36]. As it is shown in **Fig. S26**, compound C2 has shown carbon hydrogen bonds with GLN22 and CYS26. It has shown pi sigma bindings with TYR25 and TYR21, alkyl bindings with HIS27 and MET18. However, compound C4 has shown pi sigma binding with MET78 and pi sulfur with MET81 and MET55. It has shown few alkyl bindings with PRO53, LYS48, PRO49 and ILE80. But it has shown less free binding energy than C2, because of being stabilised more by aromatic compounds in active pocket of enzyme. Free binding energy of all the studied compounds are more than 5FU which has been selected as positive control. 5FU interacted 4 hydrogen bonds with VEGFA via PHE47, PHE36, and ASP34 that made it to cause stronger affinity towards VEGFA than other compounds [36].

Docking with HIF

When selenium compounds interaction was studied with HIF, all compounds showed lower binding energy than standard drug FU while C2 showed higher energy. Compound C1 contains pi-sulfur bond with MET319 and pi-sigma with VAL232. It can react and make alkyl binding with HIF in PRO229, PRO231, ARG320, VAL336 and LEU340. Compound C1 from aromatic group interacts with PRO231 and VAL336. As it is shown in **Fig. S27** of supplemantry data, the free binding energy of 5FU binds to LEU101, SER118 and GLN147 residues of HIF through conventional hydrogen bonds while compound C3 has shown pi-sigma interaction with PRO231 and VAL336. It can interact as carbon hydrogen bond with GLU323 and GLN241. Compound C3 can make alkyl bond with TYR228, PHE224, PRO229 and PHE111. Even though 5FU which has been selected as positive control has shown three hydrogen bindingswheareasneither C1 nor C3 have shown such conventional hydrogen binding;but their free binding energy is less than 5FU because of containing four and two aromatic groups respectively.Compound C2 has shown carbon hydrogen binding with PRO333 and GLU321 with length of 3.06 and 3.40 respectively while C4 has shown such binding with PRO33 with the length of 2.72, which is a shorter bond.

Conclusion

Eight N-heterocyclic compounds among them four ionic salts (L_1-L_4) and four selenium compounds (C_1–C_4) were synthesized and fully characterized through spectroscopic and chromatographic techniques. The stability studies of compounds for time period of 0, 24, 48 and 96 h in solution forms through UV-Visible spectroscopy confirmed that compounds are stable in solution form for studied period of time. Lipophilicity of compounds was in the range of log *P* (0.74–1.34) measured through shake flask method and their effect on biological activities was evaluated. The binding affinity of compounds with BSA measured in terms of K_b which found better than FDA approved antiproliferative drug cisplatin. The hemolysis of studied compounds C_1–C_4 was very less from their positive control Triton-x 100 which was an indication of safety of compounds for normal cells. The anticancer activity of compounds was measured through molecular docking studies for cancer proteins targets (COX-1, EGF, VEGF-A and HIF) as well as *In Vitro* studies for HCT-116, MCF-7 and A549 cancer cell lines. Both studies were supportive to each other for the conclusion that compounds are good cytotoxic agents.

Declaration of Competing Interest

Authors decleared no conflict of intrest on this article.

CRediT authorship contribution statement

Rizwan Ashraf: Investigation, Data curation, Writing - original draft. **Zohra Khalid:** Writing - review & editing. **Ayesha Sarfraz:** Investigation. **Haq Nawaz Bhatti:** Supervision. **Muhammad Adnan Iqbal:** Conceptualization, Methodology. **Mansoureh Nazari V:** Formal analysis, Resources.

Acknowldgment

Authors aknowldged Higher Education commission (HEC) of Pakistan for funding of project through National research program for universities-HEC via funding # NRPU-8198.

Supplementary materials

Supplementary material associated with this article can be found, in the online version, at doi:10.1016/j.molstruc.2021.130701.

References

[1] J. Sun, X. Zheng, H. Li, D. Fan, Z. Song, H. Ma, X. Hua, J. Hui, Monodisperse selenium-substituted hydroxyapatite: controllable synthesis and biocompatibility, Mater. Sci. Eng.: C 73 (2017) 596–602.
[2] M. Aouida, D. Ramotar, The budding yeast saccharomyces cerevisiae as a model system for anti-cancer drug screening, Clinics of Oncology 1 (6) (2018) 1–3.

[3] G. Spengler, M. Gajdács, M.A. Marć, E. Domínguez-Álvarez, C. Sanmartín, Organoselenium compounds as novel adjuvants of chemotherapy drugs—a promising approach to fight cancer drug resistance, Molecules 24 (2) (2019) 336.
[4] L.V. Papp, J. Lu, A. Holmgren, K.K. Khanna, From selenium to selenoproteins: synthesis, identity, and their role in human health, Antioxid. Redox Signal. 9 (7) (2007) 775–806.
[5] D. Plano, D.N. Karelia, M.K. Pandey, J.E. Spallholz, S. Amin, A.K. Sharma, Design, synthesis, and biological evaluation of novel selenium (Se-NSAID) molecules as anticancer agents, J. Med. Chem. 59 (5) (2016) 1946–1959.
[6] A. Kamal, M. Nazari, M. Yaseen, M.A. Iqbal, M.B.A. Khadeer, A.S.A. Majid, H.N. Bhatti, Green Synthesis of selenium-N-heterocyclic carbene compounds: evaluation of antimicrobial and anticancer potential, Bioorg. Chem. (2019) 103042.
[7] Z. Tian, Y. Yang, L. Guo, G. Zhong, J. Li, Z. Liu, Dual-functional cyclometalated iridium imine NHC complexes: highly potent anticancer and antimetastatic agents, Inorg. Chem. Front. 5 (12) (2018) 3106–3112.
[8] S. Aher, A. Das, P. Muskawar, J. Osborne, P. Bhagat, Silver (I) complexes of imidazolium based N-heterocyclic carbenes for antibacterial applications, J. Mol. Liq. 231 (2017) 396–403.
[9] B. Wang, L. Huang, Y. Hou, S. Lan, J. Cheng, N-Heterocyclic Carbene, NHC) Organocatalytic one-pot reaction for the enantioselective synthesis of fluoromethylated chromenones, Org. Lett. 20 (19) (2018) 6012–6016.
[10] R.L. Vekariya, A review of ionic liquids: applications towards catalytic organic transformations, J. Mol. Liq. 227 (2017) 44–60.
[11] F. El-Hajjaji, M. Messali, A. Aljuhani, M. Aouad, B. Hammouti, M. Belghiti, D. Chauhan, M. Quraishi, Pyridazinium-based ionic liquids as novel and green corrosion inhibitors of carbon steel in acid medium: electrochemical and molecular dynamics simulation studies, J. Mol. Liq 249 (2018) 997–1008.
[12] S. Fang, L. Li, B. Cui, S. Men, Y. Shen, X. Yang, Structural insight into plant programmed cell death mediated by BAG proteins in Arabidopsis thaliana, Acta Crystallographic. Sec. D 69 (6) (2013) 934–945.
[13] G. Lv, L. Guo, L. Qiu, H. Yang, T. Wang, H. Liu, J. Lin, Lipophilicity-dependent ruthenium N-heterocyclic carbene complexes as potential anticancer agents, Dalton Trans. 44 (16) (2015) 7324–7331.
[14] C. Baltazar, R. Mun, H. Tajmir-Riahi, J. Bariyanga, Spectroscopic studies on the interaction of mimosine with BSA and DNA, J. Mol. Struct. 1161 (2018) 273–278.
[15] F. Wang, Z. Yang, Y. Zhou, S. Weng, L. Zhang, J. Wu, Influence of metal ions on phosphatidylcholine–bovine serum albumin model membrane, an FTIR study, J. Mol. Struct. 794 (1–3) (2006) 1–11.
[16] D.M. Morgan, Tetrazolium (MTT) assay for cellular viability and activity, Polyamine protocols, Springer (1998) 179–184.
[17] A. Habib, M.A. Iqbal, H.N. Bhatti, A. Kamal, S. Kamal, Synthesis of alkyl/aryl linked binuclear silver (I)-N-Heterocyclic carbene complexes and evaluation of their antimicrobial, hemolytic and thrombolytic potential, Inorg. Chem. Commun. 111 (2020) 107670.
[18] A. Kamal, M. Nazari, M. Yaseen, M.A. Iqbal, M.B.K. Ahamed, A.S.A. Majid, H.N. Bhatti, Green synthesis of selenium-N-heterocyclic carbene compounds: evaluation of antimicrobial and anticancer potential, Bioorg. Chem. 90 (2019) 103042.
[19] M.A. Iqbal, R.A. Haque, W.C. Ng, L.E. Hassan, A.M. Majid, M.R. Razali, Green synthesis of mono-and di-selenium-N-heterocyclic carbene adducts: characterizations, crystal structures and pro-apoptotic activities against human colorectal cancer, J. Organomet. Chem. 801 (2016) 130–138.
[20] G. Achar, P.P. Hokrani, K. Brinda, J.G. Małecki, S. Budagumpi, Synthesis, characterization, crystal structure and antibacterial properties of N–and O–functionalized (benz) imidazolium salts and their N–heterocyclic carbene silver (I) complexes, J. Mol. Struct. 1196 (2019) 627–636.
[21] R.A. Haque, M.A. Iqbal, M.B.K. Ahamed, A.A. Majid, Z.A.A. Hameed, Design, synthesis and structural studies of meta-xylyl linked bis-benzimidazolium salts: potential anticancer agents against 'human colon cancer, Chem. Cent. J. 6 (1) (2012) 68.
[22] M. Kaloğlu, N. Kaloğlu, İ. Özdemir, S. Günal, İ. Özdemir, Novel benzimidazol-2-ylidene carbene precursors and their silver (I) complexes: potential antimicrobial agents, Bioorg. Med. Chem. 24 (16) (2016) 3649–3656.
[23] M. Atif, H.N. Bhatti, R.A. Haque, M.A. Iqbal, M.B.A. Khadeer, A.M.S.A. Majid, Synthesis, structure, and anticancer activity of symmetrical and non-symmetrical silver (I)-N-heterocyclic carbene complexes, Appl. Biochem. Biotechnol. (2020) 1–19.
[24] S. Şahin-Bölükbaşı, N. Şahin, M.N. Tahir, C. Arıcı, E. Çevik, N. Gürbüz, İ. Özdemir, B.S. Cummings, Novel N-heterocyclic carbene silver (I) complexes: synthesis, structural characterization, and anticancer activity, Inorganica Chim. Acta 486 (2019) 711–718.
[25] M. Yaqoob, S. Gul, N.F. Zubair, J. Iqbal, M.A. Iqbal, Theoretical calculation of selenium N-heterocyclic carbene compounds through DFT studies: synthesis, characterization and biological potential, J. Mol. Struct. 1204 (2020) 127462.
[26] S. Akkoç, İ.Ö. İlhan, Y. Gök, P.J. Upadhyay, V. Kayser, *In vitro* cytotoxic activities of new silver and PEPPSI palladium N-heterocyclic carbene complexes derived from benzimidazolium salts, Inorganica Chim. Acta 449 (2016) 75–81.
[27] B. Zhou, J. Song, M. Wang, X. Wang, J. Wang, E.W. Howard, F. Zhou, J. Qu, W.R. Chen, BSA-bioinspired gold nanorods loaded with immunoadjuvant for the treatment of melanoma by combined photothermal therapy and immunotherapy, Nanoscale 10 (46) (2018) 21640–21647.
[28] A. Alsalme, R.A. Khan, A.M. Alkathiri, M. Ali, S. Tabassum, M. Jaafar, H.A. Al-Lohedan, β-Carboline silver compound binding studies with human serum albumin: a comprehensive multispectroscopic analysis and molecular modeling study, Bioinorg. Chem. Appl. 2018 (2018).
[29] J. Liu, Y. He, D. Liu, Y. He, Z. Tang, H. Lou, Y. Huo, X. Cao, Characterizing the binding interaction of astilbin with bovine serum albumin: a spectroscopic study in combination with molecular docking technology, RSC Adv. 8 (13) (2018) 7280–7286.
[30] C. Pérez-Arnaiz, J. Leal, N. Busto, M.C. Carrión, A.R. Rubio, I. Ortiz, G. Barone, B. Diáz de Greñu, J. Santolaya, J.M. Leal, Role of seroalbumin in the cytotoxicity of cis-dichloro Pt (II) complexes with (N^ N)-donor ligands bearing functionalized tails, Inorg. Chem. 57 (10) (2018) 6124–6134.
[31] J. Neault, A. Novetta-Delen, H. Tajmir-Riahi, Interaction of cisplatin drug with RNase A, J. Biomolecul. Struc. Dyn. 17 (1) (1999) 101–109.
[32] H. Chen, G. Wang, L. Sun, H. Zhang, M. Sun, J. Sun, L. Shang, C. Luo, Regulating the alky chain length of fatty acid-didanosine prodrugs and evaluating its role in albumin binding, Drug Deliv. Transl. Res. 8 (1) (2018) 21–31.
[33] O.A. Chaves, V.A. da Silva, C.M.R. Sant'Anna, A.B. Ferreira, T.A.N. Ribeiro, M.G. de Carvalho, D. Cesarin-Sobrinho, J.C. Netto-Ferreira, Binding studies of lophirone B with bovine serum albumin (BSA): combination of spectroscopic and molecular docking techniques, J. Mol. Struct. 1128 (2017) 606–611.
[34] X. Liang, C. Ma, X. Yan, X. Liu, F. Liu, Advances in research on bioactivity, metabolism, stability and delivery systems of lycopene, Trends Food Sci. Technol. 93 (2019) 185–196.
[35] M.R. Reithofer, A.K. Bytzek, S.M. Valiahdi, C.R. Kowol, M. Groessl, C.G. Hartinger, M.A. Jakupec, M. Galanski, B.K. Keppler, Tuning of lipophilicity and cytotoxic potency by structural variation of anticancer platinum (IV) complexes, J. Inorg. Biochem. 105 (1) (2011) 46–51.
[36] A. Kahraman, R.J. Morris, R.A. Laskowski, A.D. Favia, J.M. Thornton, On the diversity of physicochemical environments experienced by identical ligands in binding pockets of unrelated proteins, Proteins: Struct. Funct. Bioinf. 78 (5) (2010) 1120–1136.
[37] S. Jiang, L. Zhang, D. Cui, Z. Yao, B. Gao, J. Lin, D. Wei, The important role of halogen bond in substrate selectivity of enzymatic catalysis, Sci. Rep. 6 (2016) 34750.